$^{12}C(\alpha,\gamma)^{16}O$ $E2$ cross section in a microscopic four-alpha model

P. Descouvemont
Physique Nucléaire Théorique et Physique Mathématique, Université Libre de Bruxelles, Campus Plaine, Code Postal 229, B1050 Bruxelles, Belgium
(Received 1 September 1992)

The $^{12}C(\alpha,\gamma)^{16}O$ $E2$ cross section is calculated in the generator coordinate method where ^{12}C is described by three α particles located on the apexes of an equilateral triangle. Distortion effects in the ^{12}C wave functions are taken into account, and the ^{16}O wave functions are defined by a mixing of $\alpha+^{12}C(0^+, 2^+)$ configurations. The good quantum numbers are restored through angular momentum projection. We compute quadrupole transition probabilities between low-energy ^{16}O states, and the $^{12}C(\alpha,\gamma)^{16}O$ $E2$ cross sections to the ground and 2_1^+ states. At 300 keV, we find an S factor equal to 0.09 MeV b.

PACS number(s): 25.45.−z

I. INTRODUCTION

The $^{12}C(\alpha,\gamma)^{16}O$ reaction is a key process in stellar evolution [1]. It sensitively influences the $^{12}C/^{16}O$ abundance ratio after helium burning. The determination of the cross section at astrophysical energies (typically 300 keV) is made difficult by the occurrence of two weakly bound states (1_1^- at 7.12 MeV and 2_1^+ at 6.92 MeV) located just below the $\alpha+^{12}C$ threshold in ^{16}O. These states are responsible for an enhancement of the low-energy S-factor and prevent one from a simple extrapolation of the experimental data (see Refs. [2,3] and references therein). The current data cover the energy range from 1.0 to 3.0 MeV, where the cross section is strongly affected by the broad 1_2^- (9.55 MeV) resonance. The situation is made even more complicated since the $E1$ multipolarity, which is forbidden if one neglects isospin mixing rates, is dominant near this resonance. Accordingly, the contribution of other multipolarities at low energy cannot be directly evaluated from a extrapolation of the data.

The $E2$ component of the $^{12}C(\alpha,\gamma)^{16}O$ cross section was suggested first by Dyer and Barnes [4] to be non-negligible at astrophysical energies. However, for the reasons mentioned above, this contribution was, at that time, evaluated in a very indirect way. A recent experiment [2] aimed at measuring γ-ray angular distributions and confirmed that the $E2$ component cannot be neglected. Owing to its importance in astrophysics, the $^{12}C(\alpha,\gamma)^{16}O$ has been extensively investigated in theoretical models: R-matrix fits [5–7], K-matrix fits [8], potential-model [2], semi-microscopic [9,10], and microscopic [11,12] calculations (note that we are concerned here by the $E2$ component only). All of these theoretical approaches support a significant $E2$ contribution at stellar energies. However, the quoted values for S_{E2}(300 keV) range from 0.0 to 0.18 MeV b, which represents a rather large uncertainty, compared to the precision required in nucleosynthesis studies.

The $^{12}C(\alpha,\gamma)^{16}O$ reaction is the topic of two previous microscopic investigations. In both studies, the ^{12}C nucleus is described by a one-center wave function with four $0s$ and eight $1p_{\frac{3}{2}}$ harmonic oscillator orbitals. The former calculation [11] involves the $\alpha+^{12}C(0^+)$ channel only, whereas the $\alpha+^{12}C(2^+)$, $p+^{15}N$, and $n+^{15}O$ configurations are introduced in the latter [12]. This extension of the configuration space allowed us to provide a microscopic description of the $E1$ component. Although the results obtained in Refs. [11,12] certainly provide a good estimate of the S factor [S_{E2} (300 keV) = 0.09 MeV b and 0.07 MeV b, respectively], their reliability can be partly questioned by the poor description of ^{12}C internal wave functions. The most striking evidence is that, with standard nucleon-nucleon forces, the difference between the ^{16}O and ^{12}C binding energies is much larger than experimentally observed.

The ^{12}C wave functions can be significantly improved by a triple-α description [13]. In Ref. [14] (hereafter denoted as I), we have used such antisymmetric wave functions to investigate the $\alpha+^{12}C$ system in a four-α microscopic model. In I, the ^{12}C nucleus is described by Slater determinants defined by three α particles located on the apexes of an equilateral triangle of side R^C. These basis wave functions are projected out on the 0^+ and 2^+ states of ^{12}C, and the spin and parity of $\alpha+^{12}C$ wave functions are restored through angular momentum projection. In I, attention was paid on clustering effects in ^{12}C and ^{16}O, with the investigation of ^{16}O spectroscopic properties and $\alpha+^{12}C$ phase shifts. We used different ^{12}C descriptions, corresponding to a given R^C value (0.4, 1.6, 2.8, or 4.0 fm), and showed that clustering effects in ^{12}C can be rather important in ^{16}O wave functions. Similar conclusions have been drawn recently by Fukatsu and Katō [15], who investigate the 0^+ partial wave of the $\alpha+^{12}C$ system in a semi-microscopic multicluster model.

In the present paper, we first construct $\alpha+^{12}C$ wave functions by mixing the four ^{12}C configurations mentioned above. In this case, the ^{12}C nucleus is not frozen but is allowed to be distorted during the collision. Like in I, the $\alpha+^{12}C(0^+, 2^+)$ channels are taken into account.

In a further step, we use these wave functions to compute the $^{12}C(\alpha,\gamma)^{16}O$ cross section. Of course, only the $E2$ component is accessible to such a model, since the isospin one admixtures are missing. However, the present model is expected to provide a realistic description of the $E2$ cross section which, as stated above, is still controversial. In Sec. II, we briefly present the four-α microscopic model. Section III is devoted to ^{16}O spectroscopic properties, and more especially to $E2$ transition probabilities. Capture cross sections are presented, and compared with other theoretical approaches is Sec. IV. Concluding remarks are given in Sec. V.

II. THE FOUR-α MODEL

The four-α description of the α+^{12}C system is detailed in I. Here, we only recall the main characteristics of the model and give its extension to the $E2$ multipolarity, which is not considered in I. The GCM wave function of the 16-nucleon system reads, in the partial wave $J\pi$,

$$\Psi^{JM\pi} = \sum_{\ell I} \sum_{i,j} f^{J\pi}_{\ell I}(R_i, R^C_j)\ \Phi^{JM\pi}_{\ell I}(R_i, R^C_j), \quad (1)$$

where I is the ^{12}C spin (0^+ or 2^+ in the present study) and ℓ the relative angular momentum between α and ^{12}C. In (1), $\Phi^{JM\pi}_{\ell I}(R_i, R^C_j)$ is a projected Slater determinant corresponding to a ^{12}C nucleus described by an equilateral triangle of side R^C and to an additional α particle located at distance R from the ^{12}C center of mass. The generator function $f^{J\pi}_{\ell I}(R_i, R^C_j)$ must be determined from the Schrödinger equation. In I, the sum over the R^C generator coordinate was restricted to a single value, and different wave functions (1), each corresponding to a given R^C value (0.4, 1.6, 2.8, or 4.0 fm), were used to investigate clustering effects in the α+^{12}C system. In other words, the ^{12}C wave functions were frozen since there was no mixing between the R^C values. In the present case, the sum over j in (1) runs over the four R^C values given above. As in I, the α+^{12}C generator coordinates R_i are selected from 1.1 to 8.8 fm with a step of 1.1 fm, and the oscillator parameter is taken as $b = 1.36$ fm. This choice maximizes the α binding energy with the Volkov force $V2$.

In I, details are given regarding the numerical computation of matrix elements between projected Slater determinants $\Phi^{JM\pi}_{\ell I}(R_i, R^C_j)$. These matrix elements are shown to require seven-dimensional integrals, owing to the ^{12}C and ^{16}O angular momentum projections. In this paper, we focus on the $^{12}C(\alpha,\gamma)^{16}O$ $E2$ cross section and therefore need the matrix elements of the $E2$ quadrupole operator. According to I, we have for the $\mathcal{M}^E_\lambda$ multipole

$$\begin{aligned}\langle \Phi^{J\pi}_{\ell I}(R_i, R^C_j)\ ||\mathcal{M}^E_\lambda||\ \Phi^{J'\pi'}_{\ell' I'}(R_{i'}, R^C_{j'})\rangle = 8\pi^2 \sum_{\nu\nu'\mu} &\langle J'\lambda\nu-\mu\mu|J\nu\rangle\langle \ell I 0\nu|J\nu\rangle\langle \ell' I'\nu-\nu'-\mu\nu'|J'\nu-\mu\rangle \\ &\times \int Y^0_\ell(0,0)\ D^I_{\nu,0}(\Omega)\ Y^{\nu-\nu'-\mu\star}_{\ell'}(\theta,0)\ D^{I'\star}_{\nu',0}(\Omega') \\ &\times \langle \Phi_{4\alpha}(\boldsymbol{R}_i, R^C_j, \Omega)\ |\mathcal{M}^E_{\lambda\mu}|\ \Phi_{4\alpha}(\boldsymbol{R}_{i'}, R^C_{j'}, \Omega')\rangle d\cos\theta\ d\Omega\ d\Omega'. \quad (2)\end{aligned}$$

In (2), $\Phi_{4\alpha}$ is a four-α unprojected Slater determinant, where the ^{12}C wave function is defined by an equilateral triangle with side R^C and Euler angles Ω. The vector $\boldsymbol{R}_i$ is orientated along the z axis, whereas $\boldsymbol{R}_{i'}$ makes an angle θ with respect to $\boldsymbol{R}_i$ and is located in the xz plane. As for the Hamiltonian, whose matrix elements are given in I, the $E\lambda$ matrix elements involve seven-dimensional integrals. However, computer times are lower than for the Hamiltonian since the $E\lambda$ multipole depends on one-body operators only.

The calculation of the capture cross section is performed in two steps. First, we determine the generator functions $f^{J\pi}$, with special attention to the asymptotic part of the wave function (1). Owing to the harmonic-oscillator description of the individual orbitals, the radial part of the wave function has a Gaussian asymptotic behavior. This well-known problem is solved with the microscopic R-matrix method (MRM) [16]. The second step is the calculation of the $E2$ matrix elements between the 0^+ ground state of ^{16}O and the 2^+ scattering wave of the α+^{12}C system. The definition of the capture cross section is given in Ref. [16]. The accuracy of the model can be tested through the calculation of ^{16}O spectroscopic properties, which are experimentally well known. Since the GCM provides a unified description of bound, resonant, and scattering states of a system, the reliability of spectroscopic properties, such as energy spectrum, resonance widths, or electromagnetic transitions, is an indirect test of the capture cross section.

III. SPECTROSCOPIC PROPERTIES OF ^{16}O

A. Energy spectrum

In Fig. 1, we present the GCM ^{16}O spectrum, and compare it to experiment [17]. We are here concerned with positive-parity states only, since negative-parity partial waves do not contribute to the $E2$ component of the capture cross section. In addition, they were shown in Ref. [18] to be significantly affected by isospin mixing rates. The Majorana parameter of the Volkov force V2 is $M = 0.6305$, which reproduces the binding energy of the 2^+_1 subthreshold state with respect to the α+^{12}C channel. Figure 1 shows that the ^{16}O ground state is overbound by about 12 MeV, if one fits the Majorana parameter to the 2^+_1 state. Although still rather large, this overbinding is however much lower than in "conventional" two-cluster models [11,12]. It is interesting to compare the absolute binding energy of ^{16}O, with its

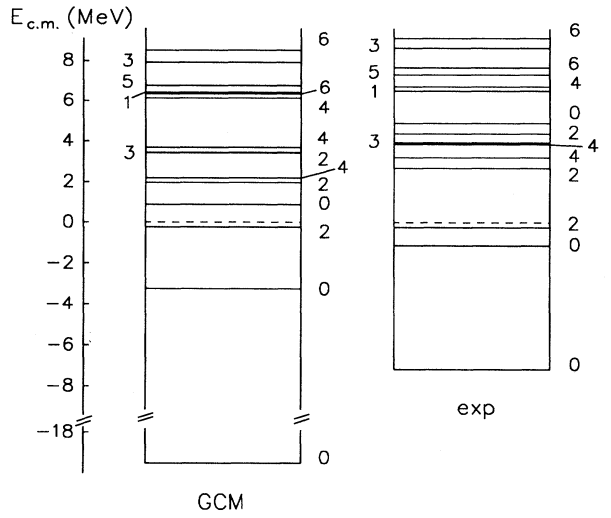

FIG. 1. GCM positive parity states, labeled by J, compared with experiment. The α+^{12}C threshold is presented as dashed lines.

counterpart obtained in the shell model. Being a closed-shell nucleus, the ^{16}O wave function is expected to be accurately described by full $0s$ and $1p$ shells. After minimization on the oscillator parameter b, one gets in the shell model: $E(^{16}\mathrm{O}) = -118.2$ MeV for $b = 1.54$ fm, and with the V2 force mentioned above. The present four-α model gives, with the same Hamiltonian, $E(^{16}\mathrm{O}) = -129.0$ MeV, which represents an improvement of about 10.8 MeV. This shows that, in the widely accepted shell-model description of ^{16}O, the binding energy is underestimated by at least 10 MeV, with respect to the exact solution of the Schrödinger equation.

Figure 1 shows that, with a nucleon-nucleon interaction common to all positive-parity partial waves, we have a satisfactory agreement with experiment. In the 0^+ partial wave, the GCM energies are too low, but the 2^+ and 4^+ experimentally known resonances are well reproduced. For non-natural-parity states, the binding energies are very close to the data.

B. $E2$ transition probabilities

As explained in Sec. I, the reliability of the model can be tested through $E2$ transition probabilities which are experimentally well known in the low-energy part of the ^{16}O spectrum. In addition, the $E2$ component of the $^{12}\mathrm{C}(\alpha,\gamma)^{16}\mathrm{O}$ cross section is very sensitive to the $B(E2, 2_1^+ \rightarrow 0_1^+)$ value. Owing to the overestimation of the ground-state binding energy, we have readjusted the 0^+ Majorana parameter in order to get the experimental value -7.16 MeV. This problem is common to all "*ab initio*" models, but the value obtained here ($M = 0.6666$) is less different from the starting value than in two-center descriptions of the α+^{12}C system [11,12]. The rms radius of the ^{16}O ground state is then 2.64 fm in the GCM, which is in reasonable agreement with experiment [17] (2.71 ± 0.02 fm).

TABLE I. $B(E2)$ in ^{16}O (expressed in W.u.).

Transition	GCM	exp [17]
$2_1^+ \rightarrow 0_1^+$	3.8	3.1 ± 0.1
$2_2^+ \rightarrow 0_1^+$	0.042	0.031 ± 0.003
$2_3^+ \rightarrow 0_1^+$	1.8	1.5 ± 0.5
$2_1^+ \rightarrow 0_2^+$	18	27 ± 3
$2_2^+ \rightarrow 0_2^+$	0.1	1.2 ± 0.3
$2_3^+ \rightarrow 0_2^+$	0.3	3.1 ± 0.5
$4_1^+ \rightarrow 2_1^+$	48	65 ± 6
$4_2^+ \rightarrow 2_1^+$	4.6	1.0 ± 0.3

In Table I, we give the $E2$ transition probabilities in ^{16}O. At this stage, there is no effective charge in the model. Table I indicates that $E2$ transitions to the ground state are very close to experiment, but the $B(E2)$ values involving the 0_2^+ state are underestimated. This is partly due to the too large binding energy of this state. Obviously, the energy difference between the 0_2^+ and 2_1^+ states, which are considered as belonging to the same α+^{12}C rotational band, remains a problem in the present model. The weak clustering in the band is also supported by the slight underestimation of the $4_1^+ \rightarrow 2_1^+$ transition probability.

IV. THE $^{12}\mathrm{C}(\alpha,\gamma)^{16}\mathrm{O}$ $E2$ CAPTURE REACTION

A. Clustering effects

Before discussing the cross section obtained with the full set of generator coordinates R^C, we first investigate clustering effects in the $^{12}\mathrm{C}(\alpha,\gamma)^{16}\mathrm{O}$ reaction by selecting a single R^C value. For each calculation, two Majorana parameters are adjusted to reproduce the binding energies of the ^{16}O ground state and the 2_1^+ subthreshold state respectively. Table II gives the conditions of the calculation, and ^{16}O spectroscopic properties relevant for $E2$ capture. It shows that the difference between the 0^+ and 2^+ Majorana parameters decreases when clustering effects are introduced in ^{12}C. As already mentioned in I, α+^{12}C clustering increases with deformation of ^{12}C, which was interpreted as a consequence of the Pauli principle. Accordingly, the reduced α width of the 2^+ state significantly increases with R^C.

The $^{12}\mathrm{C}(\alpha,\gamma)^{16}\mathrm{O}$ S factors corresponding to the different R^C values are given in Fig. 2, where we do not use any effective charge. We also present in dashed lines the GCM results obtained in the α+^{12}C(0^+) single-channel model. As is well known, the α+^{12}C(2^+) configuration is of great importance, even at low energies. The single-channel S factors are almost proportional to each other and increase according to ^{12}C clustering. They however do not present a bump near 2 MeV which is due to the 2_2^+ resonance in ^{16}O. This state has a dominant α+^{12}C(2^+) structure and, consequently, is not reproduced in a single-channel approximation. In the α+^{12}C(0^+, 2^+) approach, the low-energy S factors also depend on ^{12}C clustering. The values at the typical energy of 300 keV are given in Table II. For each theoretical $B(E2\ 2_1^+ \rightarrow 0_1^+)$, we

TABLE II. Majorana parameters, 2_1^+ reduced widths and $B(E2)$ in ^{16}O, and effective charges in $\alpha+^{12}C(0^+, 2^+)$ models with a single R^C value.

	$R^C = 0.4$ fm	$R^C = 1.6$ fm	$R^C = 2.8$ fm	$R^C = 4.0$ fm
$M(0^+)$	0.7650	0.7387	0.6809	0.6499
$M(2^+)$	0.6767	0.6625	0.6339	0.6296
$\theta_\alpha^2(2^+)$ (%)[a]	6.8	12.1	30.8	25.7
$B(E2, 2_1^+ \rightarrow 0_1^+)$ (W.u.)	3.9	5.1	4.2	6.6
$\delta e/e$	−0.11	−0.22	−0.14	−0.32
S_{E2}(300 keV) (MeV b)[b]	0.023	0.059	0.19	0.230
S_{E2}(300 keV) (MeV b)[c]	0.018	0.036	0.095	0.108

[a]Calculated at 5.4 fm.
[b]Without effective charge.
[c]With the given effective charge.

determine an effective charge which is intended to provide the experimental value 3.1 W.u. This is necessary for a meaningful comparison of the low-energy S factors. However, even after correction by the effective charge, the dependence with respect to the R^C remains rather important. With R^C lower than 2.8 fm, the S_{E2} values at 300 keV are much smaller than currently adopted (see Sec. IV C).

B. The $E2$ cross section

The ^{16}O spectrum displayed in Fig. 1 shows that, although most of the experimentally known states are fairly well reproduced by the model, the GCM energies are not accurate enough for a realistic description of the $^{12}C(\alpha,\gamma)^{16}O$ capture cross section. Furthermore, the α widths can be slightly different from experiment. Accordingly, we have used the formalism described in Ref. [12] to modify the energy and α-width of some low-energy resonances. This can be done consistently within the R-matrix theory, and provides a more accurate description of scattering wave functions at low energy. Let us briefly summarize this procedure which is detailed in Ref. [12]. The microscopic version of the R-matrix theory provides in each partial wave a large number of poles, the first ones being associated to physical ^{16}O states and the other ones simulating the background contribution. The theoretical number of poles is equal to the number of basis functions (here 64 for $J^\pi = 0^+$ and 128 for $J^\pi = 2^+$ and 4^+). Energies and reduced widths associated to these poles are obtained from GCM matrix elements and do not result from a fitting procedure. It is however easy to replace the energy or the reduced width of a pole by the experimental value if theory does not exactly agree with experiment. Of course, this procedure can be applied only if the theoretical properties of a state are close enough to experiment. Then, the correction is a consistent mixing of microscopic information with well-known experimental data. We give in Table III the GCM properties of modified poles for the $R^C = 2.8$ fm calculation and for the full-set calculation. Notice that in the $\alpha+^{12}C(2^+)$ channel, the GCM reduced widths are unchanged. For the 0^+ and 2^+ partial waves, we adopt for the pole energies the experimental resonance energies. This is of course a shortcoming since a shift is known to exist between the pole and resonance energies [7], but this shift turns out to be small for the narrow 0^+ and 2^+ resonances. In the 4^+ partial wave, a slight difference between pole and

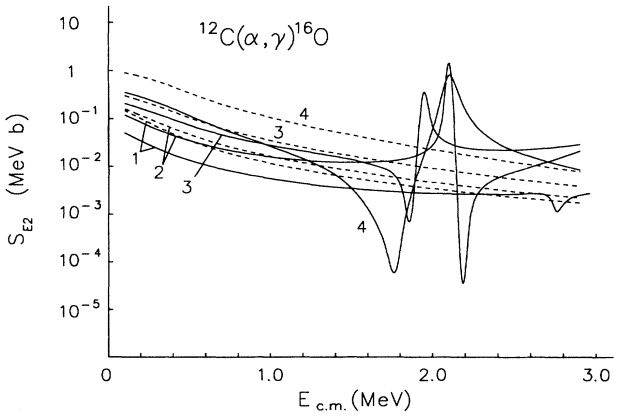

FIG. 2. $E2$ S-factors obtained with a single R^C value. Labels 1 to 4 correspond to $R^C = 0.4$, 1.6, 2.8, and 4.0 fm respectively. The dashed lines show the S-factors obtained in the $\alpha+^{12}C(0^+)$ single-channel approach.

TABLE III. Pole energies E and reduced α-widths γ (at 7.7 fm) in the 0^+, 2^+, and 4^+ partial waves. The two first columns give the GCM results and the third one gives the adopted values. The indexes refer to the pole number.

	$R^C = 2.8$ fm	mixed	adopted
$E_2(0^+)$	−2.20	−3.65	−0.11
$E_3(0^+)$	1.52	0.59	4.89
$\gamma_3(0^+)$	−0.223	−0.153	−0.012
$E_2(2^+)$	1.81	1.94	2.68
$\gamma_2(2^+)$	0.106	0.078	0.025
$E_3(2^+)$	3.53	3.17	4.36
$\gamma_3(2^+)$	0.285	0.307	0.174
$E_1(4^+)$	2.15	2.17	3.94
$E_2(4^+)$	3.69	3.63	3.00
$\gamma_2(4^+)$	−0.281	−0.208	−0.121

resonance energies must be taken into account.

The 0^+, 2^+, and 4^+ elastic phase shifts are presented in Fig. 3, with the experimental data of Plaga *et al.* [6]. The differences between the $R^C = 2.8$ fm calculation and the full calculation are negligible at low energies. This result suggests that, as soon as the internal wave functions of the colliding nuclei are realistic, distortion effects remain small. The agreement with the data indicates a satisfactory description of the background contribution.

The $E2$ S-factor relative to the ^{16}O ground state is compared to experiment in Fig. 4. Notice that, without the R-matrix correction described before, the S factor with the full set of R^C values resembles very much the S factor corresponding to R^C=2.8 fm (see Fig. 3). According to Table I, an effective charge $\delta e/e = -0.09$ is used to reproduce the experimental $2_1^+ \rightarrow 0_1^+$ transition probability. Near 2.7 MeV, the S factor is strongly affected by the 2_2^+ resonance which interferes destructively with the 2_1^+ subthreshold state. At the astrophysical energy of 300 keV, we have

$$S_{E2}\ (300\ \text{keV}) = 0.09\ \text{MeV b} \qquad (3)$$

for both ^{12}C descriptions. This value is consistent with our previous microscopic calculations (0.09 MeV b [11] and 0.07 MeV b [12]) where stronger corrections had to be made on the energy spectrum and on the effective charges. We delay until the next subsection a deeper comparison with other theoretical studies. The contribution to the S factor from capture to the 2_1^+ excited state is displayed in Fig. 5. Although presumably small, cascade transitions have been suggested by Barker and Kajino [7] to be a good tool for testing theoretical models. Figure 5 shows that the GCM S factor at 300 keV is lower than 0.01 MeV b, which is certainly lower than the uncertainties on ground-state transitions. In the experimental energy range, the GCM underestimates the data by a factor of 2. This might be an indication that $E1$ capture, due to the p wave contribution, cannot be neglected.

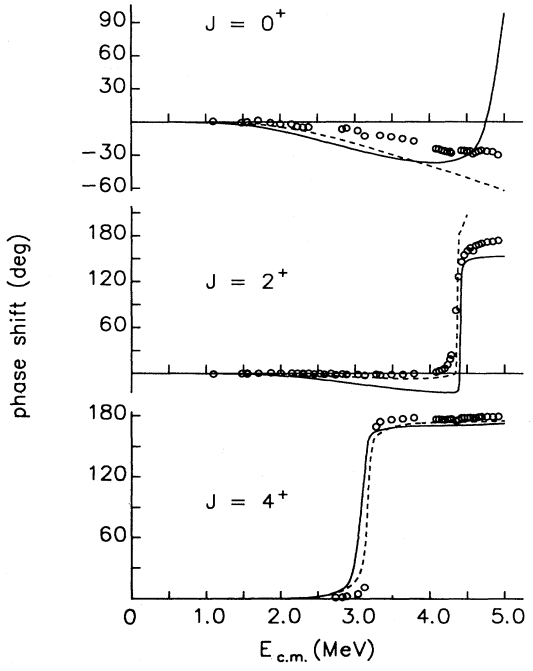

FIG. 3. α+^{12}C elastic phase shifts after the R-matrix correction explained in the text. The dashed line corresponds to a ^{12}C wave function restricted to $R^C = 2.8$ fm, whereas the full line is obtained from the mixing of four R^C values (see text). The experimental data are taken from Ref. [6].

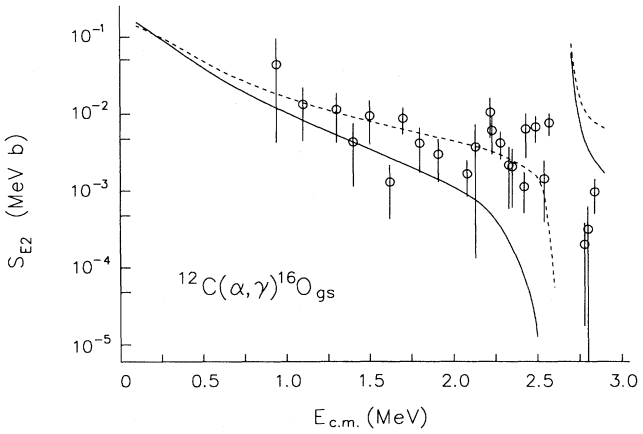

FIG. 4. $E2$ S-factors relative to the ^{16}O ground state, after the R-matrix correction explained in the text. The experimental data are taken from Ref. [6].

C. Comparison with other works

We list in Table IV the S factors at 300 keV obtained by different authors. Note that some of them are deduced from fitting procedures based on experimental data (R-matrix or K-matrix fits) whereas others are determined from *ab initio* models (GCM, OCM). In the latter approaches, experimental data are used only to test the model; all give an S-factor between 0.05 and 0.10 MeV b,

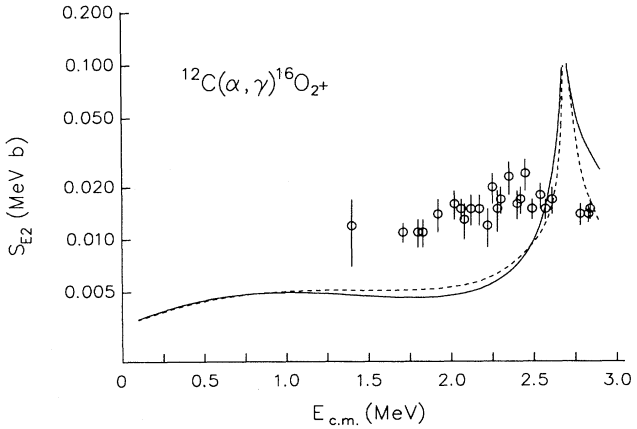

FIG. 5. See caption to Fig. 4 for capture to the 2_1^+ state.

TABLE IV. S_{E2}(300 keV) given in the literature.

Ref.	S_{E2} (MeV b)	Method
[19]	0.18	Breit-Wigner plus direct-capture models
[11]	0.09	Single-channel GCM
[10]	0.10	Single-channel orthogonality condition model
[9]	0.10	Multichannel orthogonality condition model
[2]	$0.096^{+0.024}_{-0.030}$	Three-level R-matrix fit
[2]	0.080 ± 0.025	Hybrid R-matrix fit
[2]	0.05	Single-channel orthogonality condition model
[6]	0.089 ± 0.030	R-matrix fit
[5]	$0.03^{+0.05}_{-0.03}$	R-matrix fit
[12]	0.07	Multichannel GCM
[8]	$0.007^{+0.024}_{-0.005}$	K-matrix fit
[7]	0.05 - 0.18	R-matrix fit, constrained by cascade transitions
present	0.09	Multichannel four-α GCM

which is supported by the present calculation. Fitting procedures of course sensitively depend on the availability and accuracy of experimental data. In addition, the R-matrix theory which is widely used for such fits also depends on a channel radius which cannot be determined easily. A possible constraint would be the fit of cascade transitions, as pointed out by Barker and Kajino [7]. Consequently, the S_{E2} values obtained in R-matrix fits are in general given with rather large uncertainty. In the K-matrix approach of Filippone *et al.* [8], S_{E2} is one order of magnitude lower than in the other models. We refer the reader to Ref. [7] for a detailed comparison of the R-matrix and K-matrix theories.

V. CONCLUSION

The present $E2$ S factor at 300 keV (0.09 MeV b) supports most of other *ab initio* values. The different tests on ^{12}C and ^{16}O wave functions leaves us fairly confident with our result. Of course, it only concerns the $E2$ component of the $^{12}C(\alpha,\gamma)^{16}O$ cross section. The present calculation might be extended to $E1$ capture, but should require the introduction of $T = 1$ admixtures in the wave functions. In Ref. [18], we have shown that the $^{15}N+p$ and $^{15}O+n$ configurations give a satisfactory description of isospin mixing rates and $E1$ transitions in ^{16}O. However, one should keep in mind that a four-cluster model requires the numerical evaluation of seven-dimensional integrals [14] for the computation of GCM matrix elements. Here, the occurrence of s orbitals only makes the vectorization of the codes very efficient and keeps computer times in reasonable limits. The introduction of $^{15}N+p$ and $^{15}O+n$ channels would require either p orbitals if ^{15}N and ^{15}O are defined in the one-center model, or the introduction of an additional s-shell cluster. This latter possibility is convenient for the simplicity of the codes, but necessitates computer times which are currently prohibitive.

ACKNOWLEDGMENTS

This work was supported by the Fonds National de la Recherche Scientifique. The numerical calculations have been carried out thanks to a supercomputer grant on the CRAY Y-MP of the ULB-VUB Computer Centre.

[1] C. Rolfs and W.S. Rodney, *Cauldrons in the Cosmos* (Chicago, London, 1988).
[2] A. Redder, H.W. Becker, C. Rolfs, H.P. Trautvetter, T.R. Donoghue, T.C. Rinckel, J.W. Hammer, and K. Langanke, Nucl. Phys. **A462**, 385 (1987).
[3] R.M. Kremer, C.A. Barnes, K.H. Chang, H.C. Evans, B.W. Filippone, K.H. Hahn, and L.W. Mitchell, Phys. Rev. Lett. **60**, 1475 (1988).
[4] P. Dyer and C.A. Barnes, Nucl. Phys. **A233**, 495 (1974).
[5] F.C. Barker, Aust. J. Phys. **40**, 25 (1987).
[6] R. Plaga, H.W. Becker, A. Redder, C. Rolfs, H.P. Trautvetter, and K. Langanke, Nucl. Phys. **A465**, 291 (1987).
[7] F.C. Barker and T. Kajino, Aust. J. Phys. **44**, 369 (1991).
[8] B.W. Filippone, J. Humblet, and K. Langanke, Phys. Rev. C **40**, 515 (1989).
[9] C. Funck, K. Langanke, and A. Weiguny, Phys. Lett. **152B**, 11 (1985).
[10] K. Langanke and S.E. Koonin, Nucl. Phys. **A439**, 384 (1985).
[11] P. Descouvemont, D. Baye, and P.-H. Heenen, Nucl. Phys. **A430**, 426 (1984).
[12] P. Descouvemont and D. Baye, Phys. Rev. C **36**, 1249 (1987).
[13] Y. Fujiwara, H. Horiuchi, K. Ikeda, M. Kamimura, K. Katō, Y. Suzuki, and E. Uegaki, Prog. Theor. Phys. Suppl. **68**, 29 (1980).
[14] P. Descouvemont, Phys. Rev. C **44**, 306 (1991).
[15] K. Fukatsu and K. Katō, Prog. Theor. Phys. **87**, 151 (1992).
[16] D. Baye and P. Descouvemont, Nucl. Phys. **A407**, 77 (1983).
[17] F. Ajzenberg-Selove, Nucl. Phys. **A460**, 1 (1986).
[18] P. Descouvemont, Nucl. Phys. **A470**, 309 (1987).
[19] K.U. Kettner, H.W. Becker, L. Buchmann, J. Görres, H. Kräwinkel, C. Rolfs, P. Schmalbrock, H.P. Trautvetter, and A. Vlieks, Z. Phys. A **308**, 73 (1982).